

DRUG DELIVERY INTO THE HUMAN BRAIN

A. A. Linninger*, M.B.R Somayaji, M. Xenos and S. Kondapalli.

Departments of Chemical Engineering and Bioengineering, University of Illinois at Chicago,
Chicago, IL, 60607, USA. Email: linninge@uic.edu

Abstract: Large proteins for the treatment of diseases such as Parkinson's, Alzheimer's and other disorders affecting the central nervous system (CNS) cannot easily penetrate the brain blood barrier (BBB). As an alternative to delivery through the blood stream, drugs may be inserted into the brain tissue directly using invasive release techniques. Direct injection is expected to gain importance in advanced medical treatment options such as convection-enhanced treatment of chronic diseases of the CNS, introduction of highly toxic agents in chemotherapy and gene-therapy by viral vectors. This presentation proposes a rigorous analysis of the transport phenomena effectuated by different drug release techniques. Various injection policies and effects in terms of drug perfusion rates, penetration depths and sustained drug concentrations in specific target area in the brain will be studied. Special attention will be given to studying the impact of design variables of the therapy (catheter tip, flow rate and concentration) on achievable treatment volumes. The advantages of a patient-specific approach rendering accurately the brain dimensions and physiology of each individual will be highlighted.

Keywords: Porous medium flow, human brain, drug infusion, patient-specific approach

1. Introduction

Drug delivery can be broadly classified into three different groups: (i) lipidization (pharmacological), (ii) endogenous transport and (iii) invasive methods. Pharmacological drug delivery increases the mobility of the drug so it can penetrate the BBB by conjugating water-soluble drug molecules to lipid carriers such as free fatty acids. Endogenous drug administration entails carrier-mediated (CMT) or receptor mediated transport (RMT) of macromolecules to the desired target areas in the brain (Pardridge, 1999). Invasive strategies include cerebral or ventricular infusion from intra-cerebral implants. Administering drugs into the central nervous system (CNS) poses a challenge due to the selective permeability of the capillaries in the human brain known as the "blood-brain barrier" (BBB). The BBB consists of a network of thin capillaries with special membranes protecting the brain from undesirable substances in the blood. Therefore, most proteins and high molecular weight compounds such as dyes, sucrose and catecholamines pass the BBB only with great difficulty or not at all. There are only a few clinically relevant exceptions for the treatment of neurological disorders like L-tryptophan and L-dopa capable of penetrating the blood-brain barrier (Smith and Kampine, 1984).

Invasive techniques offer a direct way of administering therapeutic drugs into targeted regions in the CNS via a catheter. (Kalyanasundaram et al., 1990, Reisfeld et al., 1995, Wang et al., 2003). The efficacy of invasive drug delivery is measured in terms of the penetration depth or treatment volume. Diffusive transport of a large molecule through the porous brain tissues depends on the free concentration gradient, the diffusivity, tortuosity of the tissue, and molecular weight of the drug. Unfortunately, diffusion alone leads to insufficient treatment volumes. *Convection enhanced delivery* (CED) is a novel approach to deliver macromolecules by imposing a convective flow field in the extra-cellular

space. CED is implemented by high flow micro-infusion of a bulk fluid (i.e. drug diluted in aqueous solution). This paper proposing an engineering approach to the design of CED is organized as follows. The background section will review briefly earlier work on invasive drug delivery. The methodology section will advocate the importance of capturing the physiological details of the target areas as well as the need for quantifying the anisotropy and inhomogeneity of the brain tissue via advanced imaging techniques. It will also introduce a two-dimensional porous medium flow model for CED based on the Navier-Stokes equations adapted for flow through a porous medium. The discussion section will offer preliminary results of a systematic parameter study affecting the drug's penetration depths such as infusate rate, drug concentration and drug diffusivity. It also studies the effects of metabolic uptake on drug delivery. Finally, a more realistic application of delivering a drug to a specific target area in the mid-brain will be illustrated. This approach reconstructs the real brain geometry of an individual patient from precise image data extracted from MR or histology.

2. Previous Work and Background

Earlier work presented experimental animal studies to identify potential drugs and policies for treating various neurological diseases (Morrison et al., 1994, Bobo et al., 1994, Hamilton et al., 2001). Morrison advocated the advantages of high flow micro-infusion. Based on a one-dimensional model for predicting the penetration depth of the drug, this author showed that slower drug degradation rates permit more effective treatment of larger brain volumes. Nicholson (1985) discussed the use of point source injection methods to describe the diffusion of a substance in the extracellular space as a function of the tissues' volume fraction, tortuosity as well as the diffusion coefficient of the drug. Kalyanasundaram et al. (1997)

proposed a chemical transport model including diffusive and convective contributions of a simplified Finite Element brain geometry in two-dimensions. The model quantified the effects of *interleukin-2* transport subject to regional differences in tissue properties, ventricular boundaries and the formation of edema. The effect of anisotropies of the CNS was also studied in a computational model mimicking the insertion of a neurotoxin into the spinal chord (Sartniranont et al, 2003). Other computational approaches to transport processes in the brain concern chemotherapy via toxin delivery by a dissolving polymer (e.g. Reisfeld et al., 1995; Wang et al., 2002). These models quantify drug diffusion and bulk flow of interstitial fluid by taking into consideration the anatomical variations in different parts of the brain.

While these studies offer insight into the selection of suitable drug molecules, a data-driven approach for CED infusion policies in human subjects still seems elusive. For a systematic approach to designing invasive drug delivery therapies, the authors of this work believe that the following issues are currently not adequately addressed by existing approaches: (i) Accurate reconstruction of the complex multi-faceted target areas of the brain. (ii) A systematic methodology for determining the dimensions and injection parameters of drug delivery equipment in humans (catheters, micro-pumps) with drug properties known from animal experiments. (iii) A computational approach to predict accurately the efficacy of chosen drug delivery parameters (injection location, angle, catheter tip, infusate flow rate, etc.). This paper aims at providing preliminary solutions to issues concerning the complex geometry of the human brain and predicting the penetration depth as a function of different drug infusion rates.

3. Methodology

3.1. Complex Brain Geometry

The complex geometry and inner organization of the brain need to be captured for transport models to be accurate. The gyrated surfaces of the cortex, the segmented three-dimensional extension, functional and physiological differentiation of the brain constitute a challenge in geometric complexity. Moreover, the key transport and metabolic parameters vary significantly in different section of the cerebrum. As an example consider the strong directional dependence of the diffusive mass transfer in the white matter along neural pathways, while in the gray matter the diffusion is almost homogenous. There are also significant individual differences in the key dimensions of the respective target areas of the CNS, making a patient-specific approach in drug delivery more significant than this is the case in the treatment of other diseases. This work proposes an accurate geometric reconstruction of the brain's inner structure from patient-specific imaging data such as magnetic resonance images (MRI) or computer tomography (CT). Although not shown in this presentation,

the proposed image-computational interface allows for the quantification of the inhomogeneous properties of the human tissue such the direction-dependent diffusivity, tortuosity, permeability and porosity.

Our *computer-assisted brain analysis* methodology starts with the collection of MR data from a powerful 3T GE Signa scanner (GE Medical Systems, Milwaukee, WI) located at the Brain Research imaging Center (BRIC) at the University of Chicago. Reconstruction tools like Mimics (Materialise Inc, 2005) convert the 3D image data into logically connected surfaces and volumes correctly interpreting abrupt changes in pixel intensities as object boundaries and interfaces. The output from the MR images reconstruction is a precise patient-specific object-oriented computational model of the brain geometry or a subsection of it. The object-oriented geometry information composed of volumes and boundary surfaces is passed into grid generator tools. The *grid generation* step segregates the geometric objects into a computational mesh with well-defined mathematical properties and specific file format. This step is also known as triangulation (Bohm et al, 2000). The computational grid composed of a fine mesh of tetrahedrons or polygons serves as input to the detailed computational analysis of transport phenomena in the brain.

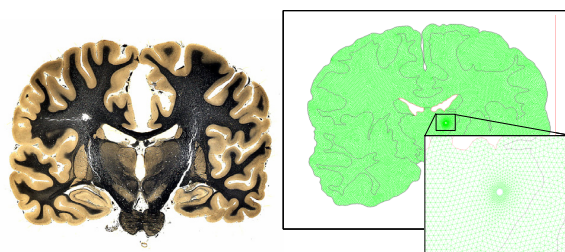


Figure 1. The detailed two-dimensional brain geometry (right) extracted from histological data (left).

The patient-specific approach described above was applied to reconstruct accurately the brain geometry e.g. gray and white matter, specific nucleus of brain subregions like Caudate Striatum and Putamen and render physiologically consistent the distribution of the complex brain inner organization. It distinguishes between gray and white matter using data extracted from histological data. Figure 1 (left) shows the histological data from which surface and shapes of the cortex, the white matter and the dimensions of the midbrain were extracted. Figure 1 (right) displays the reconstructed two-dimensional computational mesh. The detail (Figure 1 (right)) also depicts the finely resolved computational grid close to the catheter tip necessary for studying drug injection into the gray matter near the putamen.

3.2. Mathematical Model

The transport of a drug released from a catheter tip accounts for diffusion, bulk flow in a porous medium and chemical reactions, eq. (1) (Reisfeld et al, 1995).

$$\frac{\partial}{\partial t}(\rho C_i) + \frac{\partial}{\partial x}(\rho u C_i) + \frac{\partial}{\partial y}(\rho v C_i) = -\frac{\partial}{\partial x}\left(\rho D(x,y)\frac{\partial C_i}{\partial x}\right) - \frac{\partial}{\partial y}\left(\rho D(x,y)\frac{\partial C_i}{\partial y}\right) + R_i \quad (1)$$

In eq. (1) C_i is the concentration of species i in the bulk, u and v are the fluid velocity components, $D(x,y)$ is direction-dependent diffusion coefficient of the drug. The reaction terms, R_i , account for the metabolic uptake of the drug, its immobilization via receptor binding or re-absorption of the drug into the blood stream (i.e. capillary re-absorption).

$$R_i = M_i \sum_{r=1}^N \hat{R}_{i,r} \quad (1a)$$

In eq. (1a), $\hat{R}_{i,r}$ is the Arrhenius molar rate of creation or destruction of the species i in reaction r , M_i is its molecular weight. The species transport equations are coupled with bulk flow equations. The continuity equation (2) closes the mass balance for the bulk medium (i.e. water). The drug is very dilute so it does not affect the bulk flow velocities in the continuity equation. The momentum balance for the fluid are the incompressible Navier-Stokes equations ($\rho = \text{constant}$) with an additional pressure drop term accounting for the interaction of the extracellular fluid flow within a porous cell matrix, eqs (3) and (4). The terms, S_x and S_y , are more general expansions of Darcy's law known as the Forchheimer's pressure drop relation (e.g. Dullien, 1979).

Continuity of the bulk flow

$$\frac{\partial u}{\partial x} + \frac{\partial v}{\partial y} = 0, \quad (2)$$

x-momentum for fluid in porous medium

$$\rho u \frac{\partial u}{\partial x} + \rho v \frac{\partial u}{\partial y} = -\frac{\partial P}{\partial x} + \mu \left(\frac{\partial^2 u}{\partial x^2} + \frac{\partial^2 u}{\partial y^2} \right) + S_x, \quad (3)$$

y-momentum for fluid in porous medium

$$\rho u \frac{\partial v}{\partial x} + \rho v \frac{\partial v}{\partial y} = -\frac{\partial P}{\partial y} + \mu \left(\frac{\partial^2 v}{\partial x^2} + \frac{\partial^2 v}{\partial y^2} \right) + S_y, \quad (4)$$

$$S_x = -\left(\frac{\mu}{\alpha} u + \beta \frac{1}{2} \rho |u| u \right), \quad S_y = -\left(\frac{\mu}{\alpha} v + \beta \frac{1}{2} \rho |v| v \right).$$

In equations (2)-(4), u and v are the components of bulk flow velocity, ρ and μ are the infusate density and viscosity, α is the viscous resistance term equal to the inverse of permeability and β is the inertial resistance parameter. The unknowns in the transport equations (1)-(4) are the species concentration field, $C_i(x,y)$, the bulk flow

velocities u and v as well as the hydrostatic pressure field, P .

3.3. Computational approach

The transport and reaction system for drug infusion consists of a set of coupled, non-linear partial differential equations (PDEs) (1)-(4). The PDE system is discretized using a finite volume (FV) approach enforcing the conservation balances on a staggered grid expressed in generalized curvilinear coordinates (e.g. Patankar, 1980).

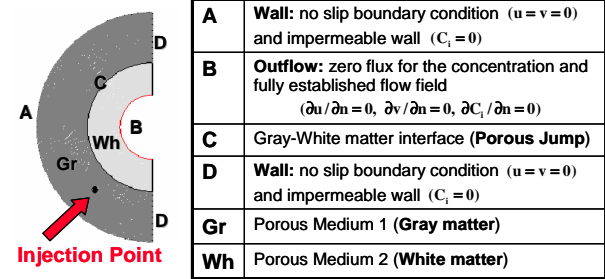


Figure 2. Boundary conditions depicted for the idealized two-dimensional brain geometry.

To complete the model, the boundary conditions shown in Figure 2 are proposed as follows. We suggest to deploy the assumption of no mass transfer across the cortex through the pia (boundary A), negligible drug transfer across the sagittal plane (boundary D) and fully established flow and concentration field across the permeable peri-ventricular area (boundary B). The inner boundary between white and gray matter constitutes a mass transfer resistance implemented as diffusion flux across a porous membrane (boundary C). The drug injection point representing the catheter tip was modeled as a small disk from which the infusate is injected with specific mass flow rate, drug concentration,

injection angle and velocity. The influence of the catheter shaft on the parenchyma is omitted in this simplified two-dimensional approach and can only be addressed properly when using a three-dimensional representation of the brain and the catheter. This extension to three dimensions, however, exceeds the scope of this paper. Clinically realistic tissue properties extracted from the literature (Morrison et al, 1994, Kalyanasundaram et al, 1997) and are summarized in Table 1.

Table 1. Parameters used

Parameter	Value
ϕ – porosity	GM 0.2 WM 0.4
k – permeability	GM 10^{+15} m^2 WM 10^{+12} m^2
β – inertia resist.	GM 10^{+4} m^{-1} WM 10^{+4} m^{-1}
μ – viscosity	0.001003 Kg/m-s
D – Drug diffusivity	$3 \times 10^{-11} \text{ m}^2/\text{s}$
GM : Gray Matter	
WM : White Matter	

4. Results and Discussion

This section studies the effect of different infusion parameters on the drug penetration depth using the mathematical approach presented in the previous section. First parameter sensitivity results will be shown in the context of a simplified brain geometry. The effects of metabolic degradation of the drug will be illustrated. A realistic problem of designing of an invasive drug treatment for a specific target area located in the mid-brain will close the computational results.

4.1. Steady State Drug infusion without metabolic uptake

Rate of Infusion. The velocity contours shown in Figure 3 depict the convective flow field as a function of the increased infusion rate. With increase of infusate flow rate convection can be enhanced as expected.

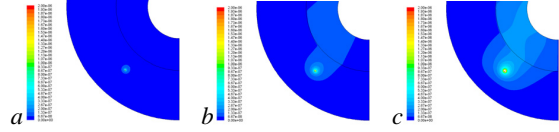


Figure 3. Velocity magnitude at different mass flow rates (\dot{m}), (from a to c convection increases).

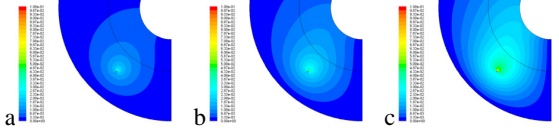


Figure 4. Drug concentration at different flow rates (\dot{m}), (from a to c convection increases).

At higher mass flow rates, the penetration depth is enhanced (Figure 4c) giving rise to a significant distribution of the drug in the white matter. At low mass flow rates diffusion dominates over convection and the penetration depth is smaller (Figure 4a).

Concentration of Infusate. These case studies simulate the impact of three different drug concentrations at a fixed infusate flow rate ($\dot{m} = 6.0 \cdot 10^{-8}$ kg/s). Higher drug concentration (C_0) leads to increased penetration depth of the drug into the porous tissue (Morrison et al, 1994). However, high concentrations near the source may be toxic for the tissues, which is certainly undesirable.

Drug Diffusivity. While larger diffusion coefficients (D) do slightly increase the penetration depth, it was found that the penetration depth is insufficient for clinical applications with diffusion alone (penetration depth < 3mm). Moreover, the result in Figure 6 shows a typical needle shaped concentration profile in pure diffusion. The establishment of a more attractive hat-shaped drug concentration profile with high concentration plateau

centered at the injection point is only possible with convection enhanced drug infusion (see Figure 6).

Table 2 summarizes the achieved drug penetration depths for the simulations without metabolic uptake. For the purpose of these parameter studies, the penetration depth is defined as the intersection of a concentration contour corresponding to a threshold level of $0.1 C_0$ with a line perpendicular to the injection direction. C_0 is the initial concentration of the drug at the catheter tip.

Table 2: Overview of simulations and penetrations

Variable	Velocity at catheter tip (m/s)	Penetration Depth (cm)
<i>(A) Rate of Infusion (\dot{m})</i>		
a Run #1 : $2.0 \cdot 10^{-8}$ Kg/s	$0.42 \cdot 10^{-5}$	~ 1.6
b Run #2 : $4.0 \cdot 10^{-8}$ Kg/s	$0.83 \cdot 10^{-5}$	~ 2.2
c Run #3 : $6.0 \cdot 10^{-8}$ Kg/s	$1.25 \cdot 10^{-5}$	~ 2.8
<i>(B) Effect of Concentration (C)</i>		
a Run #1 : $C_0 = 0.10$	$1.25 \cdot 10^{-5}$	~ 2.8
b Run #2 : $C_0 = 0.15$	$1.27 \cdot 10^{-5}$	~ 3.8
c Run #3 : $C_0 = 0.20$	$1.30 \cdot 10^{-5}$	~ 4.3

4.2. Steady State Drug infusion with metabolic uptake

This section, quantifies the effects of metabolic uptake and biodegradation of the drug. The metabolic uptake was modeled via first order kinetic occurring in the extracellular space of the brain parenchyma. For comparison, the simulation experiments and parameters described above were repeated with the addition of the reaction terms.

Rate of Infusion. First different mass flow rates were simulated. When the drug molecules are metabolized in the tissue cells the treatment volume of the drug decreases.

Concentration of Infusate. Higher drug concentrations increase the penetration depth even in the presence of metabolic reactions. The drug concentration in the extracellular space is smaller in comparison to the case without metabolic uptake due to drug consumption in the tissue.

4.3. Two-dimensional patient specific drug-delivery into the human brain

In this application, the model introduced above was extended for the design of a drug delivery problem to a specific area into a target zone near the Putamen in the mid-brain. The detailed two-dimensional brain geometry of a specific patient was extracted from a high resolution image of a caudal cross section of a human brain. Using the image reconstruction techniques described above, a computational grid consisting of a computational mesh with 21075 nodes and 37391 volumes was generated. The drug concentration profiles corresponding to three different injection scenarios (i.e. diffusion only (case a), low (case b) and high flow micro-infusion, case c) were

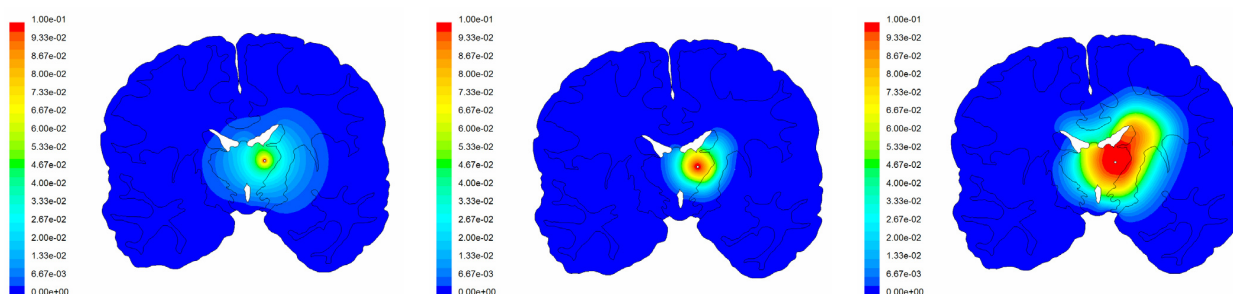


Figure 5. Diffusion (left-case a), low flow micro-infusion (middle – case b, $4.0 \cdot 10^{-8}$ Kg/s) and high flow micro-infusion of the drug (right, $8.0 \cdot 10^{-8}$ Kg/s) into the anisotropic 2D human brain.

computed using eqs (1)-(4). In all simulations, transport properties of *Table 1* were used.

Figure 5 compares the computed concentration fields which also reflect clearly the anisotropy caused by the crisscrossed pattern of white and gray matter in the mid-brain. The tissue anisotropy causes deeper drug penetration into the white than in the gray matter. Similar observations were made experimentally in small animals (e.g. Chen et al, 1999). Clearly, satisfactory treatment volumes are accomplished only via high-flow micro-infusion.

An interesting point about drug penetration can be inferred from studying drug concentration profile along a horizontal cut from point A' to A''. Figure 6 displays the characteristic hat-shaped profiles resulting from high-flow micro-infusion with a constant concentration plateau near the injection area mentioned earlier. In the pure diffusion case, the typical needles-shaped distribution emerges. It is worth mentioning that assessment of the effectiveness of the drug infusion cannot be inferred by the penetration depth alone, instead a precise quantification of the effective drug concentration in the desired target area (e.g. gray matter in the putamen) is necessary. The patient-specific application presented here allows for precise adjustment of CED treatment parameters so that effective drug delivery to a controlled region in desired concentration is ensured.

5. Conclusions

A comprehensive computer-assisted approach for assessing and designing drug delivery systems for the human brain was outlined. A methodology for the seamless integration of imaging techniques and first principles computational was demonstrated.

The key parameters affecting penetration depth of an invasive drug therapy was found to be the bulk convective velocity, which can be manipulated by the infusate rate (\dot{m}). The drug concentration at the outlet (C_0) was less significant. The diffusivity (D) appears to be the least important parameter, since only convection-enhanced transport produces clinically significant treatment volumes.

Penetration depths decreased with increased metabolic or reactive interaction of the drug with the surrounding tissue even when convection is dominant.

The detailed two-dimensional brain geometry can be extracted from MR, CT images or histological data. The simulation experiments of this patient-specific approach show the feasibility of proposed methodology to predict the achievable treatment volumes for an individual patients' specific dimensions and physiological arrangement. This capability might be also crucial for scaling-up drug therapies for humans that are based on data obtained in animals.

It is expected that better tools for studying the optimal parameter combinations for invasive drug delivery will allow physicians and scientists to develop and optimize therapeutic approaches systematically, thus reducing the need for time-consuming and often inconclusive trial-and-error animal testing.

The current approach is limited by the omission of soft tissue deformation caused by the fluid traction associated with high bulk flow velocities. It is well known that high infusion can also cause edema and other damages to the tissue. These effects are of particular importance in high flow infusion policies, which also lead to the desired hat-shaped concentration plateaus. For finding an optimal trade-off between acceptable tissue shear stresses and high penetration depths, the interaction between fluid and solid cell matrix need to be quantified. This challenge constitutes a significant future research goal.

References

- Bobo R.H., Laske D.W., Akbasak A., Morrison P.F., Dedrick R.L., Oldfield E.H., Convection-enhanced delivery of macromolecules in the brain, Proc. Natl. Acad. Sci. USA, 91(3), 2076-2080, 1991.
- Bohn G., Galuppo P., Vesnaver A.A., 3D adaptive tomography using Delaunay triangles and Voronoi polygons, Geophysical Prospecting, 48, 723-744, 2000.
- Chen M.Y., Lonser R.R., Morrison P.F., Governale L.S., Oldfield E.H., Variables affecting convection-

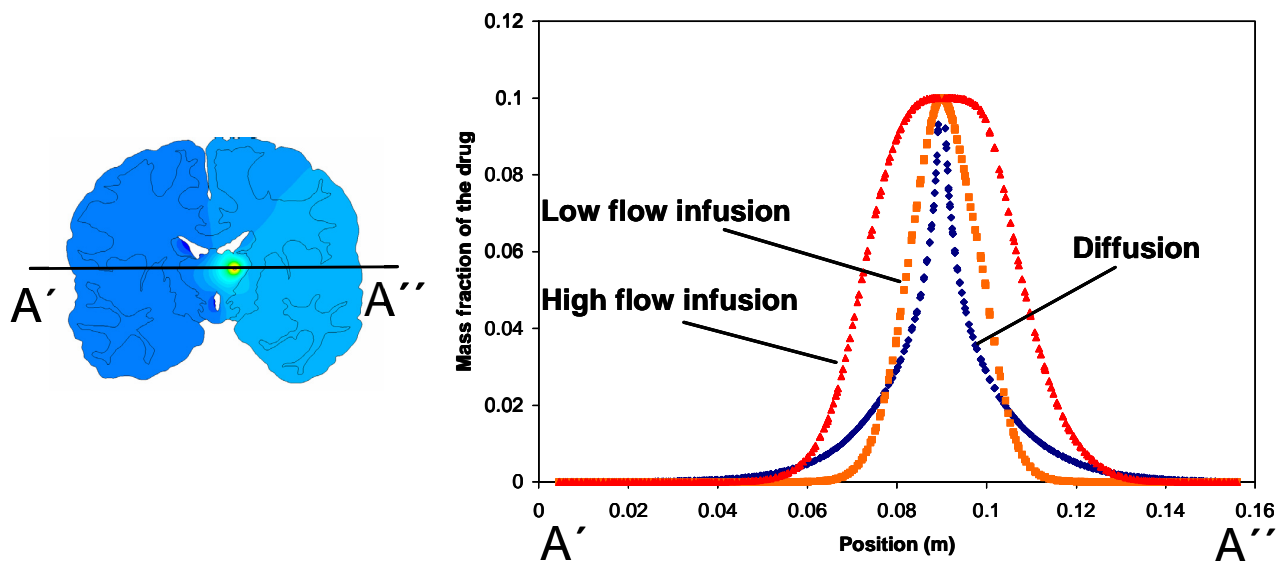


Figure 6. Mass fraction of the drug versus the position for diffusion, low and high flow micro-infusion.

- enhanced delivery to the striatum: a systematic examination of rate of infusion, cannula size, infusate concentration, and tissue-cannula sealing time, *J. Neurosurgery*, 90(2), 315-320, 1999.
- Dullien F.A.L., Porous Media, Fluid Transport and Pore Structure, Academic Press, New York, 1979.
- Hamilton J.F., Morrison P.F., Chen M.Y., Harvey-White J., Pernaute R.S., Phillips H., Oldfield E., Bankiewicz K.S., Heparin Coinfusion during Convection-Enhanced Delivery (CED) Increases the Distribution of the Glial-Derived Neurotrophic Factor (GDNF) Ligand Family in Rat Striatum and Enhances the Pharmacological Activity of Neurturin, *Experimental Neurology*, 168, 155-161, 2001.
- Kalyanasundaram, S., Calhoun, D.V., Leong, W.K., A finite element model for predicting the distribution of drugs delivered intracranially to the brain, *American Physiological Society*, R1810-R1821, 1997.
- Materialise, Inc., (Mimics), (accessed 05/30/2005) http://www.materialise.be/mimics/main_ENG.html.
- Morrison, P.F., Laske, D.W., Bobo, H., Oldfield, E.H., Dedrick, L.R., High-flow microinfusion: tissue penetration and pharmacodynamics, *American Journal of Physiology*, 266, R292-R305, 1994.
- Nagashima, T., S.T., Rapoport S I, A two-dimensional, finite element analysis of vasogenic brain edema, *Neurologia medico-chirurgica*, 30(1), 1-9, 1990.
- Nagashima T, H.B., Rapoport S I, A mathematical model for vasogenic brain edema, *Advances in neurology*, 52, 317-326, 1990.
- Nicholson, C., Diffusion from an injected volume of a substance in brain tissue with arbitrary volume fraction and tortuosity, *Brain Research*, 333, 325-329, 1985.
- Pardridge, W.M., Non-invasive drug delivery to the human brain using endogenous blood-brain barrier transport systems, *Research Focus*, 2, 2, 49-59, 1999.
- Pardridge, W.M., Drug and Gene Delivery to the Brain, The Vascular Route. *Neuron*, 36, 555-558, 2002.
- Patankar S.V., *Numerical Heat Transfer and Fluid Flow*, Series in Computational Methods in Mechanics and Thermal Sciences, W.J. Minkowycz, Sparrow, E.M., (Eds.) Washington: Hemisphere Publishing Corporation, 1980.
- Reisfeld, B., Kalyanasundaram, S., Leong, K., A mathematical model of polymeric controlled drug release and transport in the brain, *Journal of Controlled Release*, 36, 199-207, 1995.
- Sarntinoranont M., Iadarola M.J., Lonser R.R. and Morrison P.F., Direct interstitial infusion of NK₁-targeted neurotoxin into the spinal cord: a computational model, *Am J Physiol Regul Integr Comp Physiol*, 285, R243-R254, 2003.
- Smith J.J., Kampine J.P., *Circulatory Physiology, the essentials*, Williams & Wilkins, 2nd Edition, Baltimore, 1984.
- Wang, C.H., Lee, T., Tan, Wang, F., Tan, W.H.K., Simulation of Intratumoral Release of Etanidazole, Effects of the Size of Surgical Opening, *Journal of Pharmaceutical Sciences*, 92, 4, 773-789, 2003.